BJPS

Brazilian Journal of
Pharmaceutical Sciences

http://dx.doi.org/10.1590/s2175-97902023e22452

Article

Development and evaluation of wafer loaded with sertaconazole solid dispersion for the treatment of oral candidiasis

Horieh Hajhashemi[1], Somayeh Taymouri[1*], Fatemeh Shafiee[2]

[1]Department of Pharmaceutics, School of Pharmacy and Novel Drug Delivery Systems Research Centre, Isfahan University of Medical Sciences, Isfahan, Iran, [2]Department of Biotechnology, School of Pharmacy and Pharmaceutical Sciences, Isfahan University of Medical Sciences, Isfahan, Iran

Candidiasis is one of the most common fungal infections of oral cavity in humans, causing great oral discomfort, pain and aversion to food. To develop more effective antifungal systems for the treatment of oral candidiasis, an oral mucoadhesive wafer containing sertaconazole solid dispersion (STZ-SD) was developed in this study. Dispersion of STZ in Soluplus® as a solubility enhancement excipient was done by melting, solvent evaporation and freeze drying method at various STZ to Soluplus® ratios. The optimized STZ-SD was then incorporated in the sodium carboxymethyl cellulose (SCMC) gel, xanthan gum gel, or their combination to prepare the lyophilized wafers. The swelling capacity, porosity, and mechanical, release and mucoadhesive properties of the wafers, together with their antifungal activity, were then evaluated. The melting method sample with the ratio of 8:1 showed the best results in terms of saturation solubility and dissolution rate. The STZ-SD-composite wafer exhibited higher hardness and mucoadhesion, as compared to those made of the SCMC polymer. The STZ-SD-wafer also exhibited a greater antifungal effect when compared to the STZ-wafer. The present study, thus, suggested that the STZ-SD-wafer could serve as a novel effective delivery system for oral candidiasis treatment.

Keywords: Wafer, Solid dispersion. Sertaconazole. Oral candidiasis. Saturation solubility. Dissolution efficiency.

INTRODUCTION

Oral candidiasis is a common superficial human fungal infection in the oral mucosa; it is caused by the overgrowth of Candida species and characterized by whitish thick patches. *Candida albicans* (*C. albicans*) is the most frequently isolated causative pathogen of oral candidiasis (Alqarni *et al*., 2022). Although oral candidiasis is not a lethal disorder, it can cause great oral discomfort, pain and aversion to food. Therefore, it influences the patients' wellness and must be cured early to prevent chronicity, other tissues' invasion or systemic infections. Many predisposing factors such as poor nutrition, poor denture hygiene, immuno-compromised conditions such as HIV infection and cancer, endocrine dysfunction, such as diabetes mellitus, treatment with drugs such as antibacterial agents and corticosteroids, dental prosthesis, radiotherapy, and organ transplant have been identified as the factors contributing to the development of oral candidiasis. Biofilms formed by *C. albicans* are also refractory to the current treatment, thus making a reservoir for future infections (Zhang *et al*., 2017). Mouth paints, rinses, troches, lozenges, or oral gels are the current formulations available for the treatment of oral candidiasis (Alkhalidi, Hosny, Rizg, 2020; Inchara, Maheshwari, 2020; Rençber *et al*., 2016). However, dilution and rapid elimination of these formulations due to the flushing action of saliva could be regarded as the main cause of treatment failure (Komandur, Salma, Pushpalatha, 2022; Rasool *et al*., 2010; Uzunoğlu *et al*., 2021). Therefore, mucoadhesive drug delivery systems

***Correspondence:** S. Taymouri. Department of Pharmaceutics. School of Pharmacy and Novel Drug Delivery Systems Research Centre. Isfahan University of Medical Sciences, Isfahan. PO Box 81745-359, Iran. Phone: (031) 3792-7114. Email: s_taymouri@pharm.mui.ac.ir. ORCID: https://orcid.org/0000-0001-6089-8367

offer multiple benefits in treating oral candidiasis by increasing the residence time of the drug on oral mucosa and decreasing the frequency of application and the amount of the drug administered (Mura *et al.*, 2015; Hosseini, Kamali, Nabid, 2022; Hoffmann, Fischer, Daniels, 2020; Uzunoğlu *et al.*, 2021). In this context, wafers prepared by freeze-drying of mocuadhesive polymer solutions or gels yield solid porous sponge-like matrices with bioadhesive properties; they are innovative formulations that could be easily applied to mucosal surfaces for both local and systemic applications. In several studies, wafers have been developed for local and systemic drug delivery to the mucosal surfaces (Kassem, ElMeshad, Fares, 2015; El-Feky *et al.*, 2018; Sallam *et al.*, 2021). After application at mucosa, wafers are quickly turned into a gel more resistant to clearance mechanisms. In comparison with semi-solid polymeric gels, wafers can keep their swollen gel structure for a longer period of time, thus providing an increased residence time and a more effective and reproducible drug delivery (Amanat *et al.*, 2020; Barua *et al.*, 2016). In addition, they have higher drug loading capacity, as compared to the thin and denser solvent cast films, owing to their porous nature and wide surface area (Vijayan, Vipin, Kumar, 2022; Pawar *et al.*, 2014). To achieve wafers with desired properties, different hydrophilic polymers, alone or in combination, can be used (Ayensu, Mitchell, Boateng, 2012). Sodium carboxymethyl cellulose (SCMC) and xanthan gum are both polyanionic polymers considered as a suitable carrier for the delivery of drugs to moist surfaces such as buccal and nasal cavities, due to their biocompatibility, biodegradability and mucoadhesivity (Pawar *et al.*, 2014; Dehghan, Marzuka, 2014). In this study, the mixtures of SCMC with xanthan gum were used to prepare the wafer with desired characteristics.

Sertaconazole nitrate (STZ) is a potent imidazole derivate antifungal agent with a fungistatic and fungicidal effect and broad spectrum antifungal activity; it can be effective against fusarium, aspergillus, dermatophytes, yeasts of the candida and cryptococcus genera, and opportunistic filamentous fungi (Tavakoli *et al.*, 2019). STZ could selectively block ergosterol biosynthesis by inhibiting 14 α-demethylase, which could increase the permeability and membrane damage (Tavakoli *et al.*, 2019). It is also used in different skin ailments like athletes' foot and tinea pedis (Sahni, Singh, Dogra, 2018). Cream formulation containing 2 % STZ is available in the market for topical application; however, its oropharyngeal formulation has not yet been prepared in spite of its importance. In the previous studies, STZ has been shown to have the highest *in vitro* fungicidal effect against pathogenic candida clinical isolates, as compared to other antifungals such as clotrimazol, miconazole and ketoconazole (Carrillo-Muñoz *et al.*, 2013). However, STZ is practically insoluble in water, which may cause the problem of migrating through the hydrophilic base due to the lack of adequate interactions between the lipophilic drug and the hydrophilic polymer (Amanat *et al.*, 2020; Chen *et al.*, 2009; Patil *et al.*, 2021). Therefore, there is a need to develop new delivery systems capable of enhancing its aqueous solubility. Several methods have been previously used to improve the dissolution rate of poorly water soluble drugs; these include the use of surfactants, particle size reduction, salt formation, cyclodextrin inclusion complexation, solid dispersions, pH adjustment, the application of pro-drugs or incorporation of the drug in polymeric or lipid formulations (Van der Merwe *et al.*, 2020; Giri *et al.*, 2021; Kapote, Wagner, 2021). Among all, solid dispersions (SD) can be regarded as one of the simple solubilization approaches resulting from the dispersion of an active ingredient in an inert crystalline or amorphous polymer carrier (Van der Merwe *et al.*, 2020). Depending on drug properties, SD can be prepared by using fusion (melting), solvent evaporation, fusion-solvent, lyophilization and spray drying method (Alshehri *et al.*, 2020). To increase the solubility of STZ in aqueous media, different approaches have been studied; these include making complex with different cyclodextrins (Rodriguez-Perez *et al.*, 2007; Lopez-Montero *et al.*, 2009) and being incorporated into poly (Ethylene Glycol)-block-poly(ε-Caprolactone) micelles (Soliman, Attia, Mohamed, 2014). Soluplus®, polyvinyl caprolactam–polyvinyl acetate–polyethylene glycol graft copolymer is a new polymer with an amphiphilic polymer that is extensively used for fabricating the amorphous SD of insoluble drugs to improve the solubility in the aqueous media

of poorly soluble drugs (Djuris *et al*., 2013; Liu *et al*., 2020; Lamichhane *et al*., 2022; Sarpal, Munson, 2021). The eventual aim of this work was to formulate a STZ loaded SD-wafer formulation for the local delivery of STZ to treat oral candidiasis. Soluplus® was used as a drug carrier for STZ in the SD system to improve its solubility. STZ-SD was then incorporated within wafers and the obtained composites were characterized *in vitro* through the determination of hydration capacity, hardness, porosity, and bioadhesive strength. Finally, the anti-fungal activity of the best STZ-SD-wafer was evaluated *in vitro* against *C. albicans*.

MATERIAL AND METHODS

Material

STZ was purchased from Raha Pharmaceutical CO (Isfahan, Iran). Soluplus® was obtained as a gift from BASF SE (Germany). Xanthan gum, Poloxamer ®407, Poloxamer® 188, dimethylsulfoxide (DMSO), sabouraud dextrose agar and broth were purchased from Sigma Aldrich (US). SCMC, polyethylene glycol (PEG) 4000 and polyvinyl pyrolidone (PVP) k30 were bought from Merck Chemical Company (Germany). All other used chemicals and solvents were of the analytical reagent grade.

Phase solubility studies

An excess amount of the drug was added to 5 ml of water containing different increasing concentrations of PEG 4000, PVP K30, Poloxamer ®407, Poloxamer® 188 and Soluplus® (1-7.5% w/v). The samples were placed on the magnetic stirrer at 37ºC for 24 h. At predetermined intervals, an aliquot of suspensions was centrifuged at 10000 rpm for 10 min; then STZ concentration in filtrate was analyzed by a spectrophotometer at 262 nm.

Preparation of STZ-SD

Melting method

Four different amounts of Soluplus® were taken into a glass beaker and melted completely by heating up to 70 ºC. The fixed amount of STZ dissolved in a minimum amount of ethanol was then added to the molten polymer and mixed until the complete dispersion of drug occurred. The hot melted mixtures were allowed to cool at room temperature; subsequently the solidified samples were pulverized in a pestle and mortar. The prepared samples were stored in the desiccator for further studies.

Solvent evaporation method

For the preparation of STZ-SD at four different ratios, the required amounts of the drug and polymer were dissolved in a minimum amount of ethanol. The solvent was then removed at room temperature for 24 h, and the resulting residue was ground in a mortar. The prepared samples were stored in the desiccator for further studies.

Freeze drying method

For the preparation of STZ-SD at four different ratios, the required amounts of drug and polymer were dissolved in 5 cc of DMSO. The solutions were then frozen in a refrigerator at −20°C for 24 h; after that, they were lyophilized for 48 h at a temperature of −40°C and pressure of 0.001 bar by using a freeze-dryer (Christ, Alpha 2–4 LD plus, Germany).

Preparation of physical mixtures (PM)

To do the comparative solubility and dissolution study, the PM of STZ and Soluplus® with the same weight ratio, as explained in the previous three procedures, were prepared by simply mixing appropriate amounts of STZ and Soluplus® in a mortar with pestle until a homogeneous mixture was achieved. All the physical combinations were stored in the desiccator for further studies.

Characterization of the samples

Determination of saturation solubility (Cs)

The Cs of pure STZ, PM and dispersed samples was measured. 2 mg of STZ and appropriate amounts

of each SD and PM equivalent to 2 mg STZ were added to 5 mL of deionized water; stirring was done at 500 rpm and 37°C for 24 h; then the resulting suspensions was centrifuged at 10000 rpm for 10 min. Finally, the concentration of the dissolved STZ in supernatant was determined spectrophotometrically at 261 nm. Each experiment was repeated three times.

Dissolution studies

Two mg of STZ and an accurate weight of PM and STZ-SD containing 2mg of STZ were dispersed in 50 ml of a phosphate buffer solution (PBS, pH 6.8) containing 0.05 % (w/v) SLS and stirred at 400 rpm and 37°C. At specific time intervals, 0.6 ml of the samples was taken and replaced with the same fresh medium. The removed samples were centrifuged at 10000 rpm for 5 min. The amount of the dissolved STZ was quantified using a UV spectrophotometer at 261 nm. For each sample, the dissolution test was performed three times. To compare various dissolution profiles of STZ, dissolution efficiency up to 90 min ($DE_{90\ min}$ %) was calculated using the following equation:

$$DE_{90min}\% = \frac{\int_0^t y.dt}{y100.t} \times 100 \quad \text{eq.1}$$

X-ray diffraction (XRD) studies

XRD patterns of STZ, Soluplus® plain powder, PM and optimized formulation were obtained using an X-ray diffractometer (D8 ADVANCE, Bruker, Germany) with Cu Kα radiation (λ= 1.54Å). The samples were then scanned at the voltage of 40 kV and a current of 40 mA in the 2θ range of 5°-40°.

Differential scanning calorimetry (DSC)

To investigate the thermal behavior of drug and excipients used in the optimized formulation, DSC studies were performed using a DSC 822e Mettler-Toledo (Mettler Toledo, Switzerland). Samples of pure STZ, Soluplus®, STZ-SD and PM were heated at a scanning rate of 10 °C/min under nitrogen atmosphere.

Fourier transform infrared spectroscopy (FTIR)

The FTIR spectra of the selected samples were obtained using a FTIR spectrophotometer (Jasco, model 6300, Japan). Samples were prepared by potassium bromide (KBr) and scanned at wave numbers ranging from 4000 to 450 cm^{-1} with the resolution of 1.0 cm^{-1}.

Scanning electron microscopy (|SEM)

The morphology of STZ, Soluplus®, STZ-PM and STZ-SD was characterized by a LEO 1430 VP SEM (Germany). Samples were placed on an aluminum sample holder and then coated with gold using a gold sputter model in a high vacuum evaporator.

Preparation and characterization of wafer containing STZ-SD

First, 3 % (w/v) SCMC and xanthan gum gels, alone and in combination, at 1:1 weight ratio, were prepared by a homogenous dispersion of the calculated amounts of polymers in 30 ml of water under continuous magnetic stirring. STZ-SD-gel (1% w/v) was prepared by dispersing a weighed amount of STZ-SD into the gels under continuous stirring. STZ-loaded gels (1% w/v) were also prepared by the addition of an ethanolic solution of STZ to the polymeric gels for comparison. Finally, 1 g of each of the prepared gels was transferred into each well of the 24-well plates, frozen in a refrigerator at −20°C for 24 h, and then lyophilized for 48 h at a temperature of −40 ° C and pressure of 0.001 bar by applying a freeze-dryer (Christ, Alpha 2–4 LD plus, Germany).

Characterization of wafers

Mechanical properties of wafers

The mechanical properties of the wafers were measured using SANTAM instrument (SANTAM Co, Iran). Each wafer was compressed with a cylindrical stainless steel probe at a speed of 5 mm/min and to a depth of 3mm; and the magnitude of the force needed to deform the wafers was evaluated.

Swelling capacity

To determine swelling capacity, each of wafer sample was weighted (W_{Df}) and placed on a filter paper (3 cm × 3 cm) previously soaked in PBS (pH 6.8); then both of them were placed on a sponge soaked in the same medium. Sponge was put in a petri dish filled with the hydration medium to a height of 0.5 cm. At the appropriate intervals, swelling capacity was determined according to the following equation:

$$WU\ \% = \left(\frac{WHff - WHf - WDF}{WDF}\right) \times 100 \quad \text{eq.2}$$

where W_{Hff} is the weight of the hydrated wafer and wet filter, W_{Hf} is the weight of the wet filter and W_{Df} is the initial weight of the dry wafer (Abruzzo *et al.*, 2017).

Visual evaluation and scanning electron microscopy (SEM)

For visual evaluation, digital images of different formulations were captured. For the SEM study, the wafers were cut into small, thin pieces and fixed on aluminum stubs using double-sided carbon tape. After that, the wafers were gold coated using a sputter coater and examined by applying SEM.

Mucoadhesion studies

Mucoadhesive strength was determined using SANTAM instrument (SANTAM Co, Iran). For this, each formulation was attached to the surface of probe using double-sided adhesive tape. A 6.67% (w/v) gelatin gel representing the buccal mucosa surface was placed on the instrument platform. To mimic the buccal mucosa, 500 µl of PBS at pH 6.8 was spread over the surface of gelatin. Then, the probe with the attached wafers was lowered and placed on the gelatin surface for 60 sec. Finally, the maximum force required to detach the sample from the model buccal surface was determined (Farias, Boateng, 2018).

Porosity characterization

The porosity of the formulated wafers was determined by ethanol displacement method. The weighed wafers (Wi) were immersed in 10 ml of ethanol for 2 h to reach complete saturation (Wf). After that, the samples were removed from the solvent, wiped with a filter paper to remove the excess solvent and then immediately reweighed to avoid the loss of ethanol, which was volatile.

The porosity (%) of wafers was determined from following equation:

$$\text{Porosity}\% = \frac{Wf - Wi}{Pv} \times 100 \quad \text{eq.3}$$

where P is ethanol density (0.789 g/cm3) and v is the geometrical volume of wafer, which was determined by measuring the diameter and height of wafer.

In vitro drug release

For this, each wafer was immersed in beakers with 125 ml of PBS (pH=6.8) containing 0.05 % (w/v) SLS at 37°C and stirred at 400 rpm. At predetermined time intervals, 0.6 ml of the medium was taken and then replenished with the same volume of the fresh medium to maintain a constant volume. The removed samples were then centrifuged at 10000 rpm for 5 min. The amount of the dissolved STZ was quantified using a UV spectrophotometer at 261 nm (Ayensu, Mitchell, Boateng, 2012).

Determination of antifungal activity

Antifungal activities of various formulations were evaluated against *C. albicans* (PTCC5027) using the broth micro-dilution and agar diffusion method. *C. albicans* were obtained from the Persian Type Culture Collection.

In broth microdilution method, 1 ml of fungal suspension (10^5 CFU/ml), which had been prepared in sabourad dextrose broth, was poured into sterile tubes containing 9 ml of STZ, STZ- wafer and STZ-SD-wafer with various concentrations of drug (15-1000 µg/ml).The tubes were then incubated for 48 hours at 35 °C. The antifungal activity of drug free wafers was also examined, as described above, in the equivalent concentration of materials used in STZ-SD-wafer. The minimum inhibitory concentration (MIC) of each sample was determined at the end of the incubation time.

In the agar diffusion method, the fungal suspension (10^5 CFU/ml) was inoculated on sabourad dextrose agar plates; then STZ-SD-wafer and STZ-wafer containing STZ concentration to 62 µg/ml were put on the agar plate and incubated at 35 °C for 48 h. At the end of incubation, the diameter of inhibition zones was determined with a digital caliper. Drug free wafers were then used as the blank. Each test was repeated in triplicate.

RESULTS AND DISCUSSION

Phase solubility studies

Selection of a proper polymer carrier is a challenge for SD formulations, and the key in the selection of the proper solubilizer is the measurement of drug solubility in the presence of candidate polymers. Figure 1 shows the phase solubility curve of STZ in the presence of various carriers. The aqueous solubility of STZ was about 53.36±0.71 µg/ml; as can be seen, the solubility of the drug was considerably increased in the presence of the tested polymers, which could be due to the enhanced wettability of the drug. In addition, the results indicated that as the carrier concentration was increased, the solubility of STZ was raised too. Among the tested polymers, Soluplus® showed the maximum solubility of the drug. Therefore, Soluplus® was employed to prepare STZ-SD using three different methods including melting method, solvent evaporation method and freeze drying method. The weight ratio of STZ to Soluplus® was 1:1, 1:2, 1:3 and 1:4.

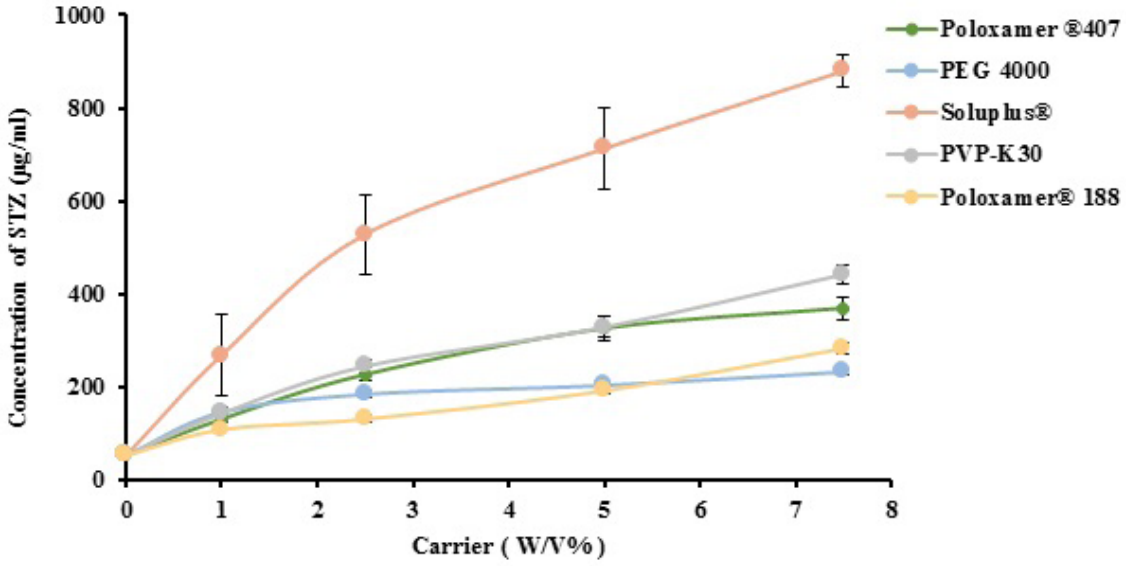

FIGURE 1 - Phase solubility curve of STZ in the presence of various carriers.

Cs and dissolution study of STZ

The results related to drug content % and dissolution tests in terms of Cs and DE for the solid dispersions at different drug to carrier ratios and their respective PM are shown in Table I. The calculated percentage of the drug content in all STZ-SDs ranged from 88.13 to 96.47%. The pure STZ showed the Cs value of 53.36 µg/ml. As can be seen, all PMs prepared by the simple mixing of the two components showed a noticeable increase in the drug solubility, as compared to STZ alone. Furthermore, raising the amount of Soluplus® in the PM systems enhanced the solubility of the STZ. These results, which were in accordance with a number of studies, could be explained by the improved wettability of the drug and solubilization properties of Soluplus® (Taymouri *et al.*, 2021). Regardless of the preparation method, except for the 2:1 ratio in the freeze drying method, other SD systems also increased the drug solubility, as compared to that of the STZ alone and PM at the same ratio, depending

on the concentration of Soluplus®. This could be due to the loss of drug crystallinity as a consequence of its almost complete molecular dispersion in the polymer, as confirmed by the subsequent solid state studies. In addition, the reduced drug particle size and the increased wettability of the drug in the presence of the hydrophilic carrier could be regarded as other possible mechanisms for the enhanced Cs solubility of STZ in SD (Adeli, 2016). As can be seen in Table I, the highest Cs of 397. 39 µg/ml was seen for the product that was made by using the melting method based on a 1:8 drug to carrier ratio, which corresponded to a 7.5 fold increase, as compared with the free drug. The dissolution curves of STZ, PM and SD in the PBS containing 0.05% w/v SLS are shown in Figure 2. All DE % values in terms of percentages are shown in Table I. As can be seen in Figure 2.a, the dissolution rate of the pure STZ was very low and only 18 % of STZ was released during 90 min. Figure 2 illustrates that the dissolution rates of all systems were significantly higher than that of the drug alone. In addition, all SDs were significantly ($p<0.001$) more effective in increasing the dissolution rate of STZ in comparison to the corresponding PM. According to the results, the formulation made via melting method with a mass ratio of 1:8 w/w caused the marked improvement in both Cs and dissolution rate. In addition, melting method is easy and takes less time. So, this formulation was selected for further investigations including XRD and DSC, as well as SEM analysis.

TABLE I - Drug content, C_S and DE for solid dispersions at different drug to carrier ratio and their respective PM

Methods	Drug/polymer ratio (w/w)	Drug content %	Dissolution efficiency %	Saturation solubility (µg/ml)
	Free STZ	**-**	**15.62 ± 2.99**	**53.36±0.71**
Solvent evaporation method				
	1:1	**92.90 ± 1.38**	**61.6 ± 1.81**	**167.35 ± 16.33**
	1:2	**96.47 ± 0.31**	**65.24 ± 1.44**	**231.54 ± 13.35**
	1:4	**94.57 ± 2.42**	**69.31 ± 2.12**	**320.64 ± 15.76**
	1:8	**90.18 ± 5.99**	**76.42± 4.75**	**372.28 ± 6.53**
Freeze Drying Method				
	1:1	**91.75 ± 2.19**	**32.49 ± 0.56**	**151.6 ± 4.80**
	1:2	**94.91 ± 1.56**	**49.44 ± 3.05**	**212.41 ± 3.85**
	1:4	**93.00 ± 0.40**	**79.20± 2.86**	**285.45 ± 6.33**
	1:8	**88.13 ± 4.77**	**95.98 ± 0.30**	**353.97 ± 16.29**
Melting Method				
	1 : 1	**94.32 ± 0.16**	**42.27± 0.19**	**193.68 ± 12.67**
	1:2	**97.62 ± 1.00**	**57.34 ± 0.50**	**231.75 ± 3.17**
	1:4	**97.17 ± 2.02**	**88.37± 3.35**	**299.24 ± 8.06**
	1:8	**94.29 ± 3.22**	**95.18 ± 4.44**	**397.39 ± 6.80**
Physical mixtures				
	1 : 1	**90.78 ± 1.56**	**20.90 ± 0.65**	**136.48± 6.17**
	1:2	**88.23 ± 3.86**	**31.98 ± 2.71**	**204.38 ± 6.17**

TABLE I - Drug content, C_S and DE for solid dispersions at different drug to carrier ratio and their respective PM

Methods	Drug/polymer ratio (w/w)	Drug content %	Dissolution efficiency %	Saturation solubility (µg/ml)
	1:4	91.61 ± 2.25	34.90 ± 1.54	253.76 ± 6.17
	1:8	86.24 ± 4.55	37.75 ± 0.52	290.80 ± 6.17

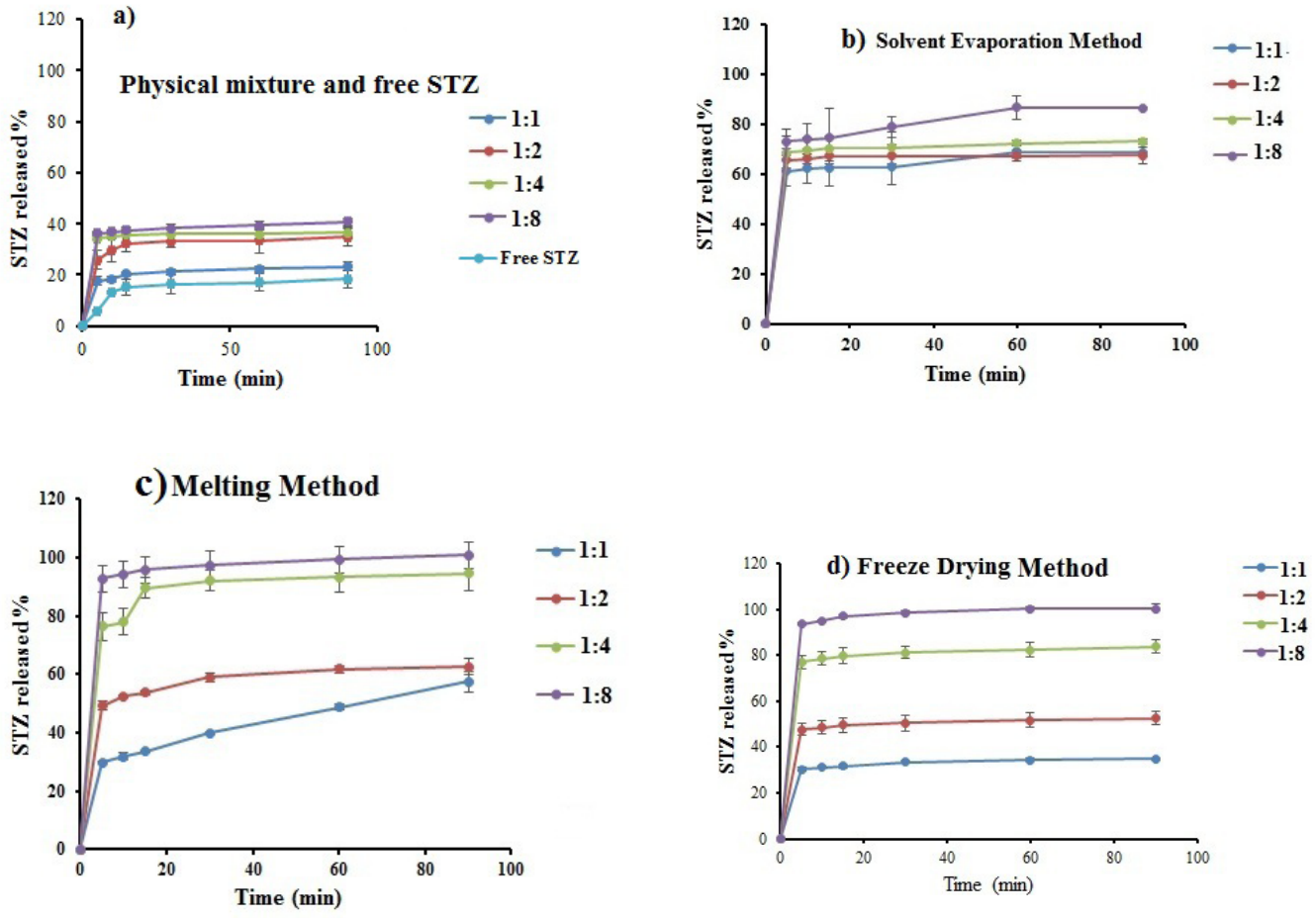

FIGURE 2 - Dissolution curves of STZ, PM and SD in PBS containing 0.05% w/v SLS.

FTIR study

To investigate the possible interaction between STZ and Soluplus® in the solid SD, the FTIR study was carried out. Figure 3 shows the FTIR spectra of STZ, Soluplus®, STZ:Soluplus® PM and STZ:Soluplus® SD. STZ showed its characteristic peaks for aromatic C–H stretching at 3,093.26 cm^{-1}, aliphatic C–H stretching at 2957.3 and 2871.49 cm^{-1}, aromatic C=C stretching at 1553.38 and 1579.41 cm^{-1}, C–N stretching at 1101–1335 cm^{-1}, and C–O–C stretching aliphatic ether at 1042-1302.68 cm^{-1} (Esenturk *et al.*, 2021). Soluplus®, on the other hand, displayed its characteristic peaks at 3457.74 cm^{-1} for O–H stretching, 2929.34 and 2859 cm^{-1} for C–H aliphatic stretching, and 1738.51 and 1639.2 $cm^{-1}$for the carbonyl stretching vibration of ester and

amide, respectively [Figure .3b]. The FTIR spectra were obtained for PM as the summation of STZ and Soluplus® individual spectra, suggesting no interactions between them in such mixtures. However, the characteristic peaks of STZ were absent in the FTIR spectrum of STZ:Soluplus® SD and only the characteristic peaks of Soluplus® could be seen. This could be due to the complete dispersion of the drug in the polymer and removal of the drug crystallinity, as also observed in a similar study (Djuris *et al.*, 2013).

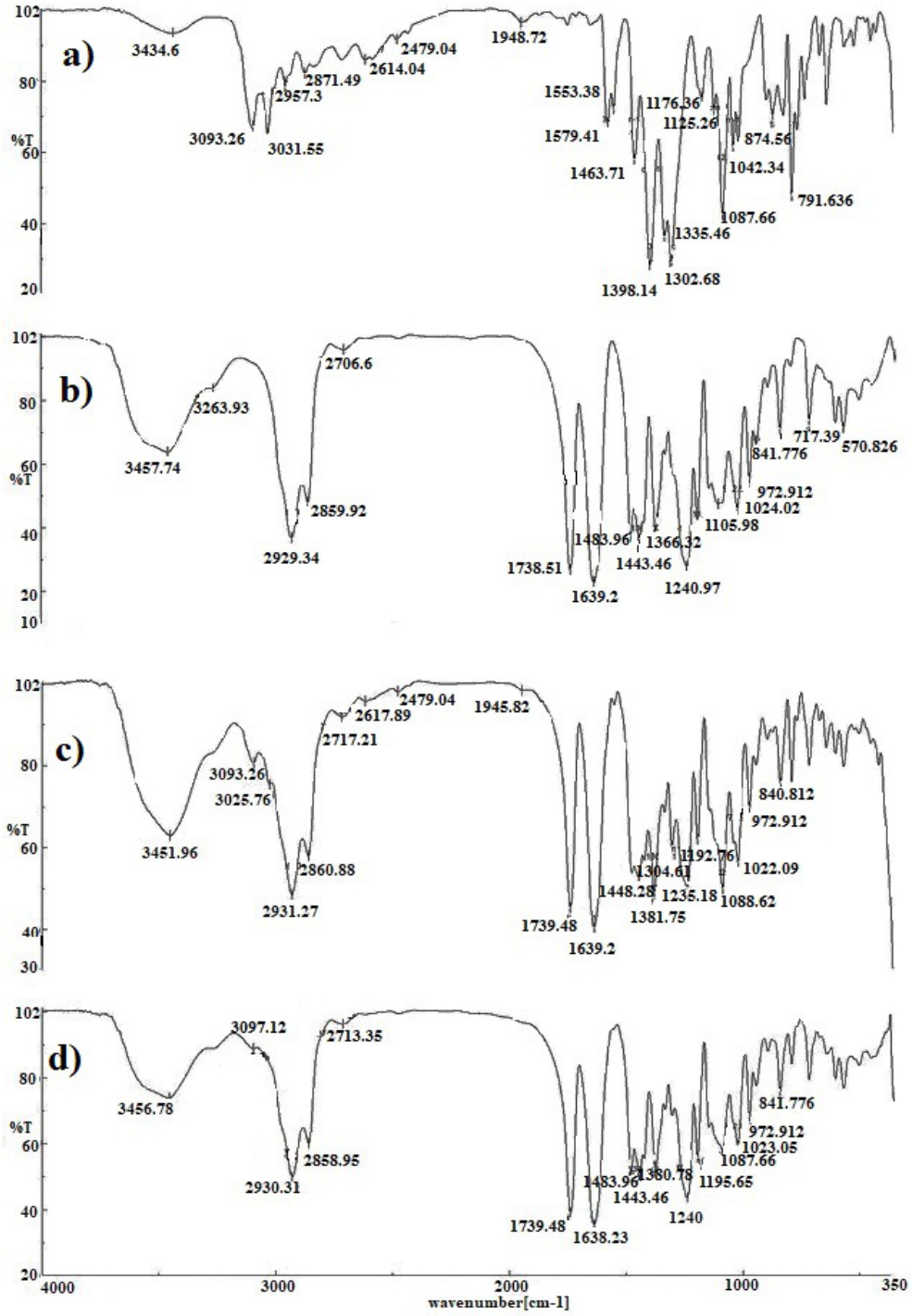

FIGURE 3 - FTIR spectra of a) STZ, b) Soluplus®, c) STZ: Soluplus® PM and d) STZ: Soluplus® SD.

XRD study

The solid state of the drug in SD was evaluated using XRD studies. The XRD patterns of STZ, Soluplus®, STZ: Soluplus® PM and STZ: Soluplus® SD are displayed in Figure 4. The raw STZ showed high-intensity peaks at 2θ values of 15.45, 17.1, 18.85, 19.8, 20.9, 23.15, 24.6, 26.12, 26.55, 28.15 and 29.35, indicating the crystalline nature of STZ (Figure.4a), while Soluplus® displayed a halo pattern because of its amorphous nature (Figure. 4b). STZ: Soluplus® PM showed less intense peaks, which were possibly due to the dilution effect of the polymer (Figure.4c). This, thus, indicated that STZ had retained its crystalinity in the PM mixture. In the case of STZ: Soluplus® SD (Figure.4d), the characteristic peaks of STZ completely disappeared, thus indicating that STZ turned into the amorphous state in STZ: Soluplus® SD.

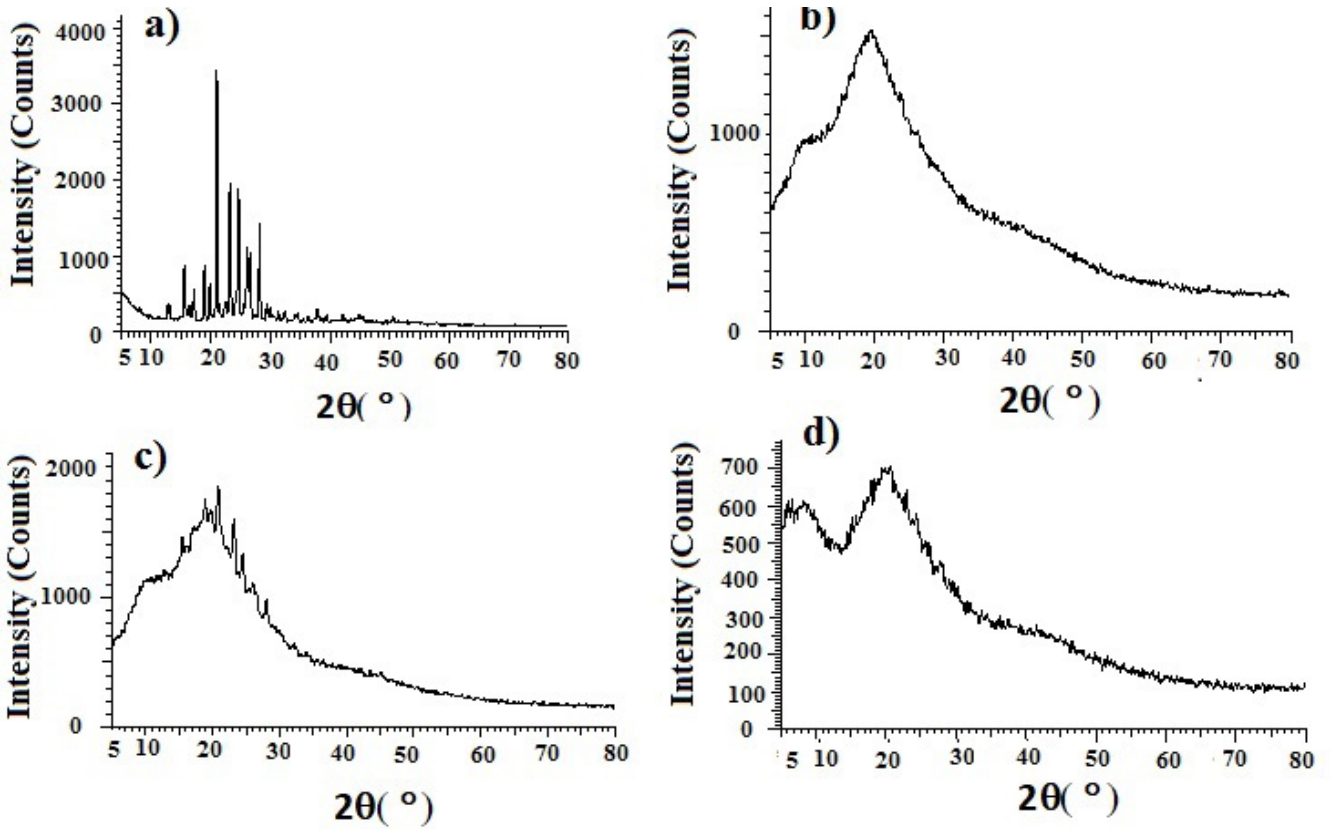

FIGURE 4 - XRD of a) STZ, b) Soluplus®, c) STZ: Soluplus® PM and d) STZ: Soluplus® SD.

DSC thermograms

The DSC thermograms of STZ, Soluplus®, STZ: Soluplus® PM and STZ: Soluplus® SD are shown in Figure 5. The curve for STZ displayed an endothermic peak at 162.1 °C, indicating the melting point of the drug (Figure.5a). On the other hand, the DSC curve of Soluplus® showed a broad endothermic peak at 82.2° C that corresponded to its glass transition (Figure 5b). Meanwhile, the curves for STZ: Soluplus® PM showed a weak endothermic peak in the melting region of the drug, thus indicating that the simple mixtures still had the crystallinity of STZ (Figure.5c). However, in the thermograms of STZ-SD, no endothermic peaks around the melting point of crystalline STZ was seen (Figure.5d). This showed that STZ changed into an amorphous form with the disappearance of crystallinity.

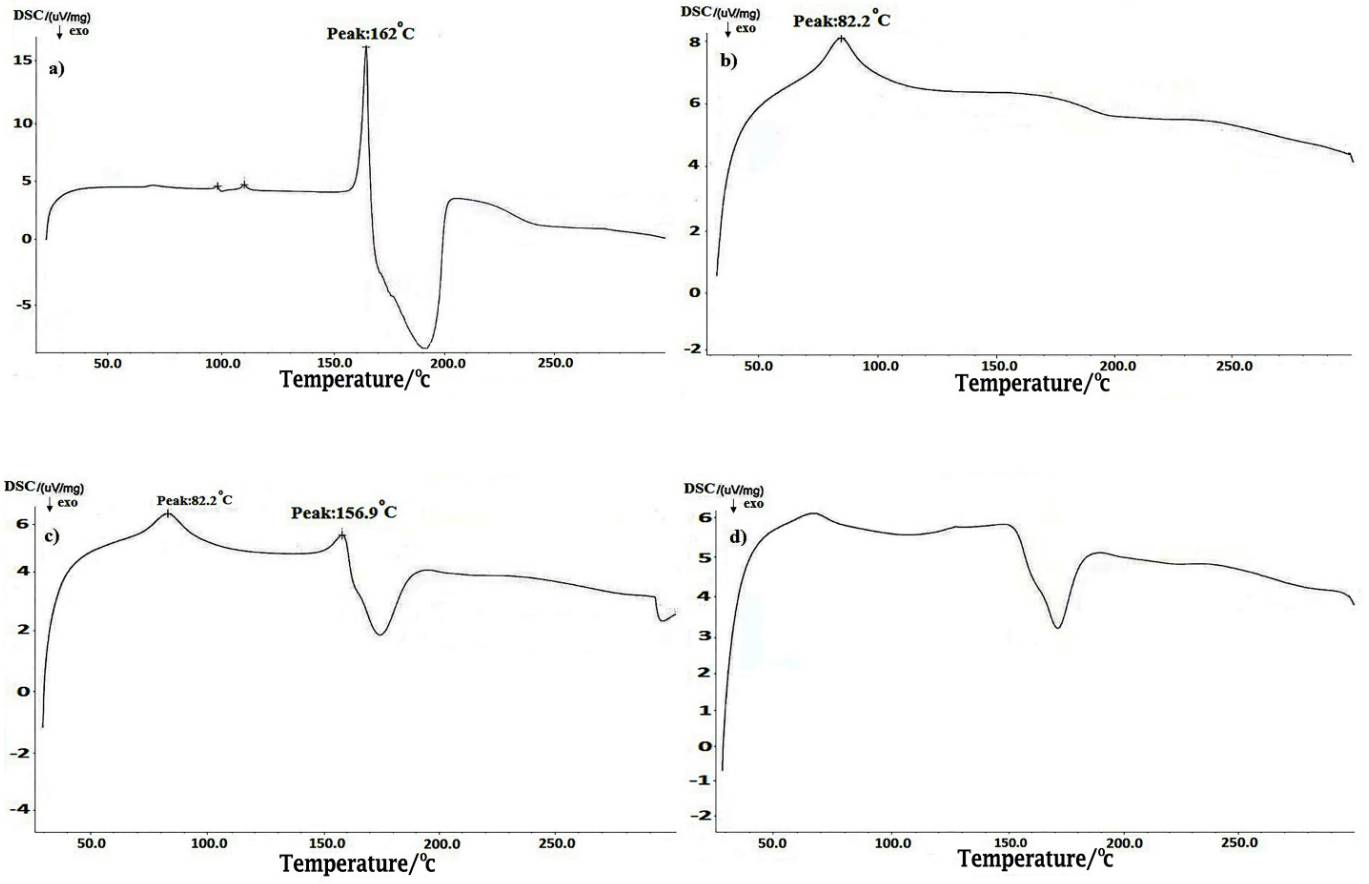

FIGURE 5 - DSC thermograms of a) STZ, b) Soluplus®, c) STZ: Soluplus® PM and d) STZ: Soluplus® SD.

SEM analysis

The morphological characteristics of STZ, Soluplus®, STZ-PM and STZ-SD were evaluated by SEM. The results are shown in Figure 6. STZ was observed as plate-like crystals, indicating a crystalline form (Figure .6a). Irregular shaped particles of Soluplus® can be seen in Figure 6b. In the SEM images of PM, smaller dug crystals were visible (Figure.6c). However, in the image of STZ-SD, irregular, round shaped particles with no sharp crystal of STZ were observed (Figure.6d). This indicated that upon preparation of SD, the crystalline form of STZ was successfully disrupted, uniformly distributed in the matrix and transformed to an amorphous form; this was in line with the results of XRD and DSC.

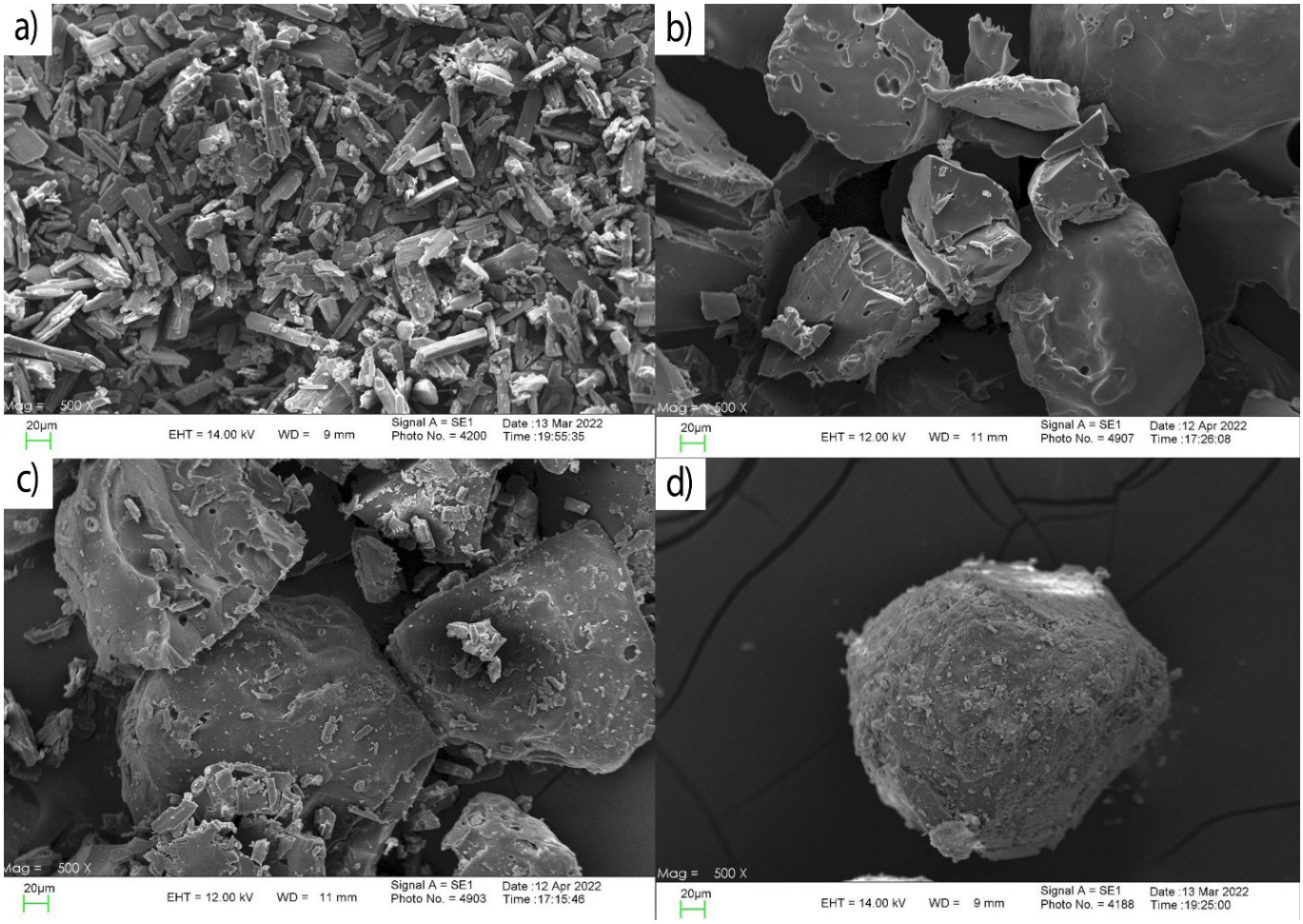

FIGURE 6 - SEM images of a) STZ, b) Soluplus®, c) STZ-PM and d) STZ-SD.

Wafer development and optimization

Various wafers containing only SCMC, xanthan gum and their combination at the weight ratio of 1:1 were prepared and examined for physicochemical properties. Digital photographs of the freeze-dried wafers formulated are shown in Figure.7a. It could be observed that SCMC and composite wafers were flexible and possessed a smooth surface with a uniform texture and thickness, thus making them suitable for easy application and potentially, patient's compliance. In contrast, xanthan gum gels formed sponges with rough and puffy-like surface. Hence, xanthan gum wafer was excluded from the study and only wafers prepared using SCMC, and SCMC/ xanthan gum were selected for further evaluation. Table II shows hardness, porosity %, adhesive strength and release efficiency of the formulated wafers. Hydration capacity of a buccal adhesive system is a key property influencing the release rate of drug (Okeke, Boateng, 2017). As shown in Figure.7b, SCMC wafers were found to have higher swelling capacity with a maximum of 352.94% during 3 h, as compared with the composite wafer. On the other hand, the combination of the polymers caused a decrease in the swelling of wafers. Differences in the porosity and hardness of wafers appear to affect the rate of water ingress into wafers (Farias, Boateng, 2020). The higher porosity of the SCMC wafer could result in the faster liquid transport (Table II). On the contrary, the liquid transport measured for the composite wafers was slower, possibly due to its lower porosity, as compared to the SCMC wafers (Table II). In addition, the hydration capacity is always negatively correlated to hardness (Farias, Boateng, 2020). The composite wafer showed the higher hardness when compared

with SCMC wafers. The higher hardness of composite wafer may cause the lower hydration capacity of wafers (Farias, Boateng, 2020; Amanat *et al*., 2020) and could be explained by increased hydrogen bonding interaction between SCMC and xanthan gum, resulting in denser solid matrix and less porous structure and therefore, water ingress within the wafer. Mucoadhesive performance of a buccal adhesive system is another physical property evaluated in our study, since it determined the residence time of formulations at the absorption site to allow for the sustained drug release and ultimately, bioavailability (Ayensu, Mitchell, Boateng, 2012), which were influenced by flexibility, molecular weight, presence of chemical groups, hydrogen binding capacity, charge, concentration and hydration of polymers (Hanafy, Leporatti, El-Kemary, 2019). It could be evidently seen from Table II that in the case of the composite wafer, higher bioadhesive strength was obtained, as compared to CMC wafers. This could be due to the presence of negatively charged carboxyl groups in the backbone of both xanthan gum and SCMC, which promoted the increased formation of strong hydrogen bonds between the polymer functional groups and the mucosal layer (Tasdighi, Azar, Mortazavi, 2012). Figure.7c shows the release profiles of STZ from various formulated wafers. As shown, the wafer sustained the release of STZ, as compared to STZ-SD. However, the release rate of STZ-SD-Wafer was faster than that of STZ-Wafer. In addition, the rate of STZ release from SCMC wafers was faster, as compared to the composite wafers. The rapid release of the SCMC wafers corresponded to its higher swelling index, which could be regarded as the main factor affecting the rate of the drug release from the wafers (El-Feky *et al*., 2018). The slower release of STZ from the composite wafers, which corresponded to its lower swelling index, helped to achieve the sustained release of STZ to decrease the need for frequent administration. Since the microstructure of wafers can influence their physical properties, such as their hydration, hardness and ultimately, drug release behavior (Rezvanian, Tan, Ng, 2016), the morphological characteristics of freeze dried wafers were evaluated by SEM. The results are shown in Figure.7d. The micrograph obtained from the SEM showed that the formulated wafers possessed an interconnected porous network with a sponge-like morphology. The SEM images were in accordance with the porosity results. As can be seen, the composite wafer was more compact than the SCMC one, which was more porous. According to the above results, the composite wafer was selected for antifungal investigation as it showed the highest mucoadhesion and hardness, and more sustained release profiles, as compared to other wafers

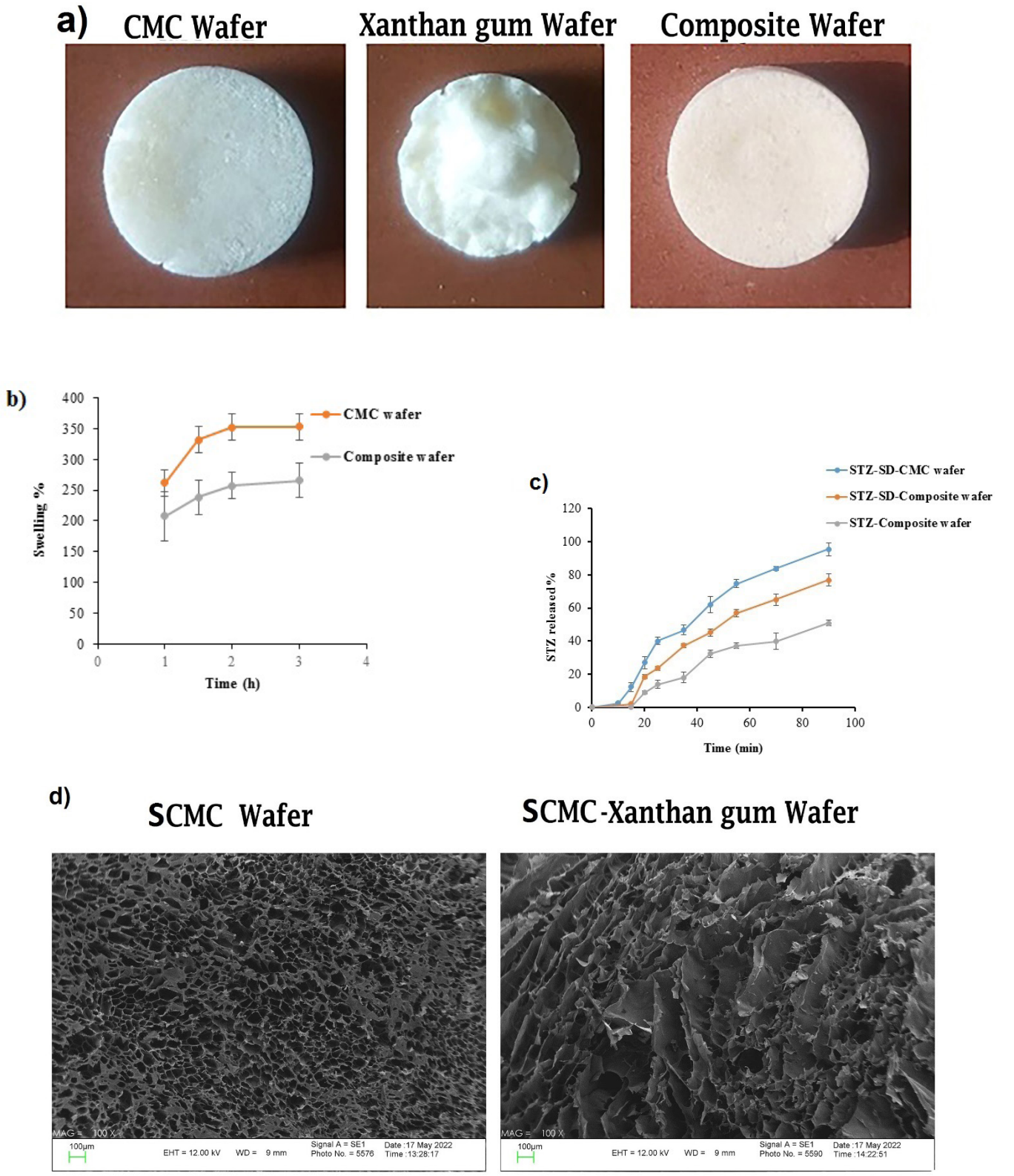

FIGURE 7 - a) Digital photographs of different formulated freeze-dried wafers, b) Swelling profiles of different formulated freeze-dried wafers, c) Release profiles of STZ from various formulated wafers and d) SEM images of different formulated freeze-dried wafers.

TABLE II - Physicochemical characterization of the formulated wafers

Formulations	Hardness (N)	Adhesive strength (N)	Porosity %	Release efficiency %
Composite wafer	**69.15±5.84**	**0.62 ± 0.02**	**56.27 ± 1.21**	**41.44 ± 1.89**
SCMC wafer	**43.47 ± 1.09**	**0.47 ± 0.03**	**76.89 ± 4.68**	**55.15 ± 2.40**

In vitro antifungal study

In this study, the MIC of STZ, STZ-wafer, STZ-SD-wafer and drug free wafer was evaluated using the microdilution effect; this was 0.210±0.070, 0.187±0.088, 0.062±000 and 0.833 ±0.289 mg/ml, respectively. According to the obtained data, the lowest concentration without growth of *C. albicans* was obtained for the STZ-SD-wafer, as compared to other groups, which could be due to the quick release of the drug from the polymeric matrix after SD was incorporated. The zone and diameter of the inhibition zone of *C. albicans* in the presence of the STZ-SD-wafer, STZ-SD and the drug-free wafer were 10 ± 0 mm, 6.3 ± 1.1 mm and 0, respectively. According to Figure 8, the drug-free wafer did not show any zone of inhibition. However, a clear zone was seen for STZ-wafer and STZ-SD-wafer. Furthermore, the mean diameter of the zone of inhibition for the STZ-SD-wafer was larger than that of the STZ-wafer. Overall, the higher MIC and zone of inhibition of the STZ-SD-wafer indicated that this formulation could be beneficial in the buccal delivery of STZ and it could increase the therapeutic efficacy in comparison to the free STZ.

FIGURE 8 - The zone and diameter of inhibition zone of *C. albicans* in the presence of STZ-SD-wafer, STZ-SD and drug free wafer.

CONCLUSIONS

In this work, a novel buccoadhesive lyophilized wafer loaded with STZ-SD was successfully developed. The results showed that the use of Soluplus® in the dispersed formulations led to the significant enhancement of Cs and dissolution rate in a concentration dependent manner. Of all formulated SDs, the melting sample at the ratio of 1:8 was selected to be incorporated in wafer, showing the highest dissolution rate and Cs, as compared with other samples. Further, it was found that xanthan gum in combination with SCMC as a gel forming matrix

was superior to SCMC polymer alone due to the enhanced mucoadhesion and hardness, as well as more prolonged release profile. Since the solubility was amplified, the wafer containing STZ-SD demonstrated a greater antifungal effect against *C. albicans, as* compared to the STZ-wafer. Therefore, the STZ-SD-wafer could be an efficient candidate for the treatment of oral candidiasis. However, further clinical studies are needed to fully explore the potential of this system.

ACKNOWLEDGMENTS

The authors wish to thank the Research Vice Chancellery of Isfahan University of Medical Sciences for supporting this work

DECLARATION OF CONFLICTING INTERESTS

The authors report no conflicts of interest.

REFERENCES

Alqarni MH, Foudah AI, Alam A, Salkini MA, Muharram MM, Labrou NE, et al. Development of Gum-Acacia-Stabilized Silver Nanoparticles Gel of Rutin against Candida albicans. Gels. 2022;8(8):472.

Alkhalidi HM, Hosny KM, Rizg WY. Oral gel loaded by fluconazole–sesame oil nanotransfersomes: development, optimization, and assessment of antifungal activity. Pharmaceutics. 2020;13(1):27.

Alshehri S, Imam SS, Hussain A, Altamimi MA, Alruwaili NK, Alotaibi F, et al. Potential of solid dispersions to enhance solubility, bioavailability, and therapeutic efficacy of poorly water-soluble drugs: newer formulation techniques, current marketed scenario and patents. Drug Deliv. 2020;27(1):1625-43.

Ayensu I, Mitchell JC, Boateng JS. Development and physico-mechanical characterisation of lyophilised chitosan wafers as potential protein drug delivery systems via the buccal mucosa. Colloids Surf B. 2012; 91:258-65.

Abruzzo A, Nicoletta FP, Dalena F, Cerchiara T, Luppi B, Bigucci F. Bilayered buccal films as child-appropriate dosage form for systemic administration of propranolol. Int J Pharm. 2017;531(1):257-65.

Adeli E. Preparation and evaluation of azithromycin binary solid dispersions using various polyethylene glycols for the improvement of the drug solubility and dissolution rate. Braz J Pharm Sci. 2016;52:01-13.

Amanat S, Taymouri S, Varshosaz J, Minaiyan M, Talebi A. Carboxymethyl cellulose-based wafer enriched with resveratrol-loaded nanoparticles for enhanced wound healing. Drug Deliv Transl Res. 2020;10(5):1241-54.

Ayensu I, Mitchell JC, Boateng JS. Development and physico-mechanical characterisation of lyophilised chitosan wafers as potential protein drug delivery systems via the buccal mucosa. Colloids Surf, B. 2012;91:258-65.

Barua S, Kim H, Jo K, Seo CW, Park TJ, Lee KB, et al. Drug delivery techniques for buccal route: formulation strategies and recent advances in dosage form design. J Pharm Investig. 2016;46(7):593-613.

Carrillo-Muñoz AJ, Tur-Tur C, Giusiano G, Marcos-Arias C, Eraso E, Jauregizar N, et al. Sertaconazole: an antifungal agent for the topical treatment of superficial candidiasis. Expert Rev Anti-Infect Ther. 2013;11(4):347-58.

Chen MC, Tsai HW, Liu CT, Peng SF, Lai WY, Chen SJ, et al. A nanoscale drug-entrapment strategy for hydrogel-based systems for the delivery of poorly soluble drugs. Biomaterials. 2009;30(11):2102-11.

Dehghan MH, Marzuka M. Lyophilized chitosan/xanthan polyelectrolyte complex based mucoadhesive inserts for nasal delivery of promethazine hydrochloride. Iran J Pharm Sci. 2014;13(3):769.

Djuris J, Nikolakakis I, Ibric S, Djuric Z, Kachrimanis K. Preparation of carbamazepine–Soluplus® solid dispersions by hot-melt extrusion, and prediction of drug–polymer miscibility by thermodynamic model fitting. Eur J Pharm Biopharm. 2013;84(1):228-37.

El-Feky GS, Farouk Abdulmaguid R, Zayed GM, Kamel R. Mucosal co-delivery of ketorolac and lidocaine using polymeric wafers for dental application. Drug Deliv. 2018;25(1):35-42.

Esenturk I, Gumrukcu S, Özdabak Sert AB, Kök FN, Döşler S, Gungor S, et al. Silk-fibroin-containing nanofibers for topical sertaconazole delivery: preparation, characterization, and antifungal activity. Int J Polym Mater Polym Biomater. 2021;70(9):605-22.

Giri BR, Kim JS, Park JH, Jin SG, Kim KS, Din FU, et al. Improved bioavailability and high photostability of methotrexate by spray-dried surface-attached solid dispersion with an aqueous medium. Pharmaceutics. 2021;13(1):111.

Farias S, Boateng JS. Development and functional characterization of composite freeze dried wafers for potential delivery of low dose aspirin for elderly people with dysphagia. Int J Pharm. 2018;553(1-2):65-83.

Farias S, Boateng JS. In vitro, ex vivo and in vivo evaluation of taste masked low dose acetylsalicylic acid loaded composite wafers as platforms for buccal administration in geriatric patients with dysphagia. Int J Pharm. 2020;589:119807.

Hosseini MS, Kamali B, Nabid MR. Multilayered mucoadhesive hydrogel films based on Ocimum basilicum seed mucilage/thiolated alginate/dopamine-modified hyaluronic acid and PDA coating for sublingual administration of nystatin. Int J Biol Macromol. 2022;203:93-104.

Hoffmann A, Fischer JT, Daniels R. Development of probiotic orodispersible tablets using mucoadhesive polymers for buccal mucoadhesion. Drug Dev Ind Pharm. 2020;46(11):1753-62.

Hanafy NA, Leporatti S, El-Kemary MA. Mucoadhesive hydrogel nanoparticles as smart biomedical drug delivery system. Appl Sci. 2019;9(5):825.

Inchara R, Maheshwari TU. In situ gel treatment for oral mucosal lesions: A systematic review. Int J Oral Health. 2020;12(6):499.

Komandur K, Salma U, Pushpalatha C. Formulation of a Ginger Extract Liquid Bandage and Assessing Its Antimicrobial, Anti-Inflammatory, and Antioxidant Efficacy: An In-Vitro Study. *ECS Trans.* 2022;107(1):19217.

Kapote DN, Wagner KG. Influence of shellac on the improvement of solubility and supersaturation of loratadine amorphous solid dispersion using a new grade of HPMC. J Drug Deliv Sci Technol. 2021;61:1021-16.

Kassem MA, ElMeshad AN, Fares AR. Lyophilized sustained release mucoadhesive chitosan sponges for buccal buspirone hydrochloride delivery: formulation and in vitro evaluation. AAPS PharmSciTech. 2015;16(3):537-47.

Lopez-Montero E, Santos JF, Torres-Labandeira JJ, Concheiro A, Alvarez-Lorenzo C. Sertaconazole-Loaded Cyclodextrin–Polysaccharide Hydrogels as Antifungal Devices. Open Drug Deliv J. 2009;3(1).

Liu P, Zhou JY, Chang JH, Liu XG, Xue HF, Wang RX, et al. Soluplus-mediated diosgenin amorphous solid dispersion with high solubility and high stability: development, characterization and oral bioavailability. Drug Des Dev Ther. 2020;14:2959.

Lamichhane S, Seo JE, Keum T, Noh G, Bashyal S, Cho SW, et al. Enhancing solubility and bioavailability of coenzyme Q10: formulation of solid dispersions using Soluplus® as a carrier. Arch Pharm Res. 2022;45(1):29-37.

Mura P, Mennini N, Kosalec I, Furlanetto S, Orlandini S, Jug M. Amidated pectin-based wafers for econazole buccal delivery: Formulation optimization and antimicrobial efficacy estimation. Carbohydr Polym. 2015;5;121:231-40.

Okeke OC, Boateng JS. Nicotine stabilization in composite sodium alginate based wafers and films for nicotine replacement therapy. Carbohydr Polym. 2017;155:78-88.

Patil M, Bhagade P, Amale M, Sonawane S, Kshirsagar S. Development of sertaconazole nitrate loaded nanostructured lipid carriers gel using central composite design: In vitro and Ex vivo evaluation. Nanosci Nanotechnol - Asia. 2021;11(1):132-43.

Pawar HV, Boateng JS, Ayensu I, Tetteh J. Multifunctional medicated lyophilised wafer dressing for effective chronic wound healing. J Pharm Sci. 2014;103(6):1720-33.

Rasool BK, Abu-Gharbieh EF, Awni RA, Rasool AA. In vitro release study of nystatin from chitosan buccal gel. Jordan J Pharm Sci. 2010;3(1):44-55.

Rençber S, Karavana SY, Yılmaz FF, Eraç B, Nenni M, Özbal S, et al. Development, characterization, and in vivo assessment of mucoadhesive nanoparticles containing fluconazole for the local treatment of oral candidiasis. Int J Nanomed. 2016;11:2641.

Rezvanian M, Tan CK, Ng SF. Simvastatin-loaded lyophilized wafers as a potential dressing for chronic wounds. Drug Dev Ind Pharm. 2016;42(12):2055-62.

Rodriguez-Perez AI, Rodriguez-Tenreiro C, Alvarez-Lorenzo C, Concheiro A, Torres-Labandeira JJ. Sertaconazole-HPβCD-pluronic F127 solid inclusion complexes: characterization and effect on drug solubility. J Incl Phenom Macrocycl Chem. 2007;57(1):497-501.

Sallam NM, Sanad RA, Ahmed MM, Khafagy EL, Ghorab M, Gad S. Impact of the mucoadhesive lyophilized wafer loaded with novel carvedilol nano-spanlastics on biochemical markers in the heart of spontaneously hypertensive rat models. Drug Deliv Transl Res. 2021;11(3):1009-36.

Sahni K, Singh S, Dogra S. Newer topical treatments in skin and nail dermatophyte infections. Indian Dermatol Online J. 2018;9(3):149.

Sarpal K, Munson EJ. Amorphous Solid Dispersions of Felodipine and Nifedipine with Soluplus®: Drug-Polymer Miscibility and Intermolecular Interactions. J Pharm Sci. 2021;110(4):1457-69.

Soliman GM, Attia M, Mohamed R. Poly (ethylene glycol)-block-poly (ε-caprolactone) nanomicelles for the solubilization and enhancement of antifungal activity of sertaconazole. Curr Drug Deliv. 2014;11(6):753-62.

Tasdighi E, Azar ZJ, Mortazavi SA. Development and in-vitro evaluation of a contraceptive vagino-adhesive propranolol hydrochloride gel. Iran J Pharm Res. 2012;11(1):13.

Tavakoli N, Taymouri S, Saeidi A, Akbari V. Thermosensitive hydrogel containing sertaconazole loaded nanostructured

lipid carriers for potential treatment of fungal keratitis. Pharm Dev Technol. 2019;24(7):891-901.

Taymouri S, Ahmadi Z, Mirian M, Tavakoli N. Simvastatin nanosuspensions prepared using a combination of pH-sensitive and timed-release approaches for potential treatment of colorectal cancer. Pharm Dev Technol. 2021;26(3):335-48.

Uzunoğlu B, Wilson CG, Sağıroğlu M, Yüksel S, Şenel S. Mucoadhesive bilayered buccal platform for antifungal drug delivery into the oral cavity. Drug Deliv Transl Res. 2021;(1):318-27.

Vijayan A, Vipin CL, Kumar GV. Dual growth factor entrapped nanoparticle enriched alginate wafer-based delivery system for suppurating wounds. Int J Biol Macromol. 2022;208:172-81.

Van der Merwe J, Steenekamp J, Steyn D, Hamman J. The role of functional excipients in solid oral dosage forms to overcome poor drug dissolution and bioavailability. Pharmaceutics. 2020;12(5):393.

Zhang P, Yang X, He Y, Chen Z, Liu B, Emesto CS, et al. Preparation, characterization and toxicity evaluation of amphotericin B loaded MPEG-PCL micelles and its application for buccal tablets. Appl Microbiol Biotechnol. 2017;101(19):7357-70.

Received for publication on 02nd July 2022
Accepted for publication on 22st November 2022